

Design and Optimization of Control Strategy to Reduce Pumping Power in Dynamic Liquid Cooling

Rajesh Kasukurthy

Department of Mechanical and Aerospace Engineering,
The University of Texas at Arlington,
Arlington, TX 76019
e-mail: rajesh.emnspc@gmail.com

Amruthavalli Rachakonda¹

Department of Mechanical and Aerospace Engineering,
The University of Texas at Arlington,
Arlington, TX 76019
e-mail: amruthav.rachakonda@gmail.com

Dereje Agonafer

Presidential Distinguished Professor
Department of Mechanical and Aerospace Engineering,
The University of Texas at Arlington,
Arlington, TX 76019
e-mail: agonafer@uta.edu

Data centers are a large group of networked servers used by organizations for computational and storage purposes. In 2014, data centers consumed an estimated 70 billion kWh in the United States alone. It is incumbent on thermal engineers to develop efficient methods in order to minimize the expenditure at least toward cooling considering the limited available power resources. One of the key areas where electronic cooling research has been focusing, is addressing the issue of nonuniform power distribution at the rack, server and even at package levels. Nonuniform heating at the chip level creates hotspots and temperature gradients across the chip which in turn significantly increases the cost of cooling, as cooling cost is a function of the maximum junction temperature. This challenge has increased the use of temperature sensing mechanisms to help in finding ways to mitigate the gradients. A very effective way to conserve pumping power and address hotspots on the single or multichip modules is by targeted delivery of liquid coolant. One way to enable such targeted delivery of coolant is by using dynamic cold plates coupled with self-regulating flow control device that can control flow rate based on temperature. This novel technology will have more effective implementation coupled with a good control strategy. This paper addresses the development and testing of such control strategy with minimal sensors along with less latency and optimization of the same.

[DOI: 10.1115/1.4049018]

Keywords: direct liquid cooling, dynamic cold plates, flow control device, energy efficiency, pumping power savings

1 Introduction

A data center is a facility composed of networked computers and storage that businesses or other organizations use to organize, process, store, and disseminate large amounts of data. A business typically relies heavily upon the applications, services, and data contained within a data center, making it a focal point and critical asset for everyday operations [1]. Due to the rapid increase in business and industries, there is an increase in demands of processing and storage of data. Increasing demands of processing and storage of data cause a corresponding increase in power density of servers. Because of this ever-increasing demand, the data center cooling costs are constantly on the rise as they need large amounts of energy for cooling. Due to this huge energy consumption by data center facilities, operators have placed a significant emphasis on the energy efficiency of the building's overall operation.

Both direct and indirect forms of liquid cooling offer many advantages such as higher heat capacities and lower transport energy requirements over conventional air cooling. A lot of work on direct liquid cooling has shown that it is also a feasible solution for IT cooling [2–4]. In the indirect methods, using water as a cooling medium through cold plates or rear door heat exchangers is a good example of the demonstration of the benefits of a liquid cooling strategy [5–7]. With single-phase liquid cooling utilizing cold plates, efficiency of the cooling system can be increased with elevated coolant supply temperatures and possible use of waste heat for other applications [8]. Cold plates have been a long-standing method of bringing water cooling to high powered devices such as the IBM's thermal conduction module (TCM) of the

late 1970s [9]. Sources such as ASHRAE TC 9.9 [10] provide ample data and guidelines for implementing water-cooled data center environments. Indirect liquid cooling not only increases cooling efficiency but also reliability of the hardware. Multichip modules that house several functional units on the same die can create hotspots due to nonuniform heat distribution on the module [11]. The large temperature gradients created across the module can negatively affect the performance and reliability of the module. Using conventional cold plates often results in over-usage of resources, as the cost for cooling is directly proportional to the maximum junction temperature observed at any point across the entire module.

A viable solution for this is using dynamic cold plate (DCP). A DCP has sections with individual inlets and outlets that allows for targeted delivery of coolant to specific regions of the module. This can help considerably cut down on pumping requirements [11]. Using individual pumps for each of its sections that relies on an array of temperature sensors to identify temperatures on various regions of the module will increase the complexity. Studies have shown that centralized pumping will have more efficiency than distributed pumping [12–15]. The use of a heat sensitive flow control device (FCD) negates the need for individual pumps and temperature sensors thereby further increasing pumping-power savings and operation reliability. The necessity of numerous temperature and pressure sensors, a suitable control system and the maintenance and reliability issues that they manifest, can be significantly minimized with the use of a *self-sensing* and controlling smart FCD. This paper discusses about the control strategy that can be adapted by using one of such self-sensing and controlling FCDs.

2 Computational Fluid Dynamics Setup and Procedures

2.1 Model for Testing Controls. To have a good energy saving model, control strategy plays an important role besides cold

¹Corresponding author.

Contributed by the Electronic and Photonic Packaging Division of ASME for publication in the JOURNAL OF ELECTRONIC PACKAGING. Manuscript received January 14, 2020; final manuscript received October 27, 2020; published online January 19, 2021. Assoc. Editor: Saket Karajgikar.

plates and FCDs. This is implemented on a rack level using a computational fluid dynamics (CFD) model in 6SigmaET. A rack level system with direct liquid cooling uses water to carry the heat away from the cold plates. A properly designed cold plate not only have high heat transfer performance but also minimal pressure drop across itself, as higher pressure drop results in increased pumping power. The schematics in Fig. 1 show four standard channel cold plates connected in parallel representing the cold plate sections. FCD is attached at the outlet of the cold plate which will regulate the flow rate based on the temperature. In this study, FCD is just a damper that changes the percentage of opening. The pressure sensors monitor the pressure drop across the cold plate. There are pressure sensors at the beginning of inlet and ending of outlet manifolds to monitor the overall pressure drop across the system. The flow rate sensors will help in monitoring the flow for each cold plate. Inlet temperature of the coolant is kept constant. Inlet and outlet are connected to a pump boundary condition that mimics the pump settings.

2.2 Integration of MATLAB With 6SigmaET. A control system is developed in MATLAB that is integrated with 6SigmaET which provides the customized controls of the damper according to the FCD functionality. The controller will change the opening area of the damper to regulate the coolant flow rate based on the

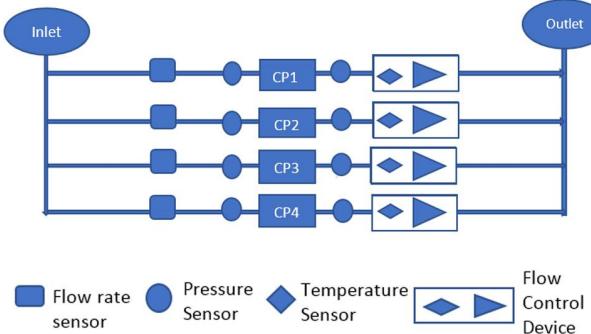


Fig. 1 Schematic representation of CFD analysis

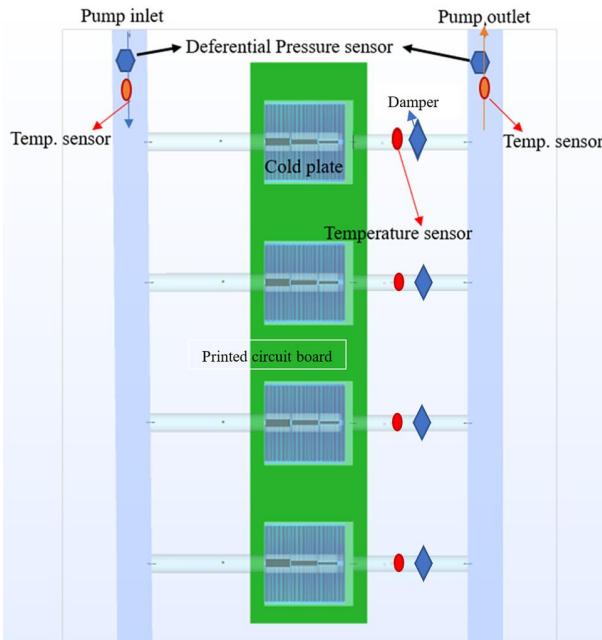


Fig. 2 Model in 6SigmaET

temperature sensor that is attached to it as shown in Fig. 2. Dead Band width is set as 0.1°C to have high accuracy. Every iteration will report the temperature values to MATLAB using solver exchange and the output from the code is sent back to the solver as new inputs. All the MATLAB integrations performed are embedded from solver exchange methodology of the 6Sigma user manual. Figure 2 shows the model in 6SigmaET. This model uses smart objects in the software tool to build the setup. The green board is a printed circuit board (PCB) object in 6SigmaET. The blue tubes are duct objects in 6SigmaET. A pump boundary condition is attached at the inlet and outlet to supply the required flow rate of coolant.

A 400-W component with a square inch area is assumed for the study with a cold plate attached to cool it. All the power generated by the component is dissipated through the cold plate into the coolant. The coolant will maintain the component temperature below the specifications of the component which is less than 100°C . Component temperatures are not reported as they are proportional to the flow rate and temperature rise of the coolant. The coolant considered in this study is water and the flow rate will be controlled by MATLAB controls.

2.3 MATLAB controls. A constant pressure-based control strategy is tested with variable frequency drive (VFD) pump. This type of pumps will save energy by reducing the electricity consumption. The flowchart shown in Fig. 3 shows that the pressure difference across the system will be taken into MATLAB and processed as shown based on the set point value. The set point value such as pressure and total flow rate is dependent on the system and varies from system to system. A MATLAB code for FCD is created and integrated with 6SigmaET to test the control strategy and a distinct code is designed specially to control the pump by sensing the pressure changes in the system.

2.4 Computational Fluid Dynamics. The equations that govern the motion of a Newtonian fluid are the continuity equation, the Navier–Stokes equations, and the energy equation. The set of equations listed below represents seven equations that are to be satisfied by seven unknowns [16,17]. The scope of our analysis predominantly lies in the laminar region of flow owing to low flow velocities and relatively simple geometries. The only instance where a k-Epsilon turbulence model is used is in the region between when the damper is completely closed and when it is open by an angle of 10 degs. The equations used for solving in the laminar as well as turbulent regions are listed below [18]. As shown in Eqs. (1) through (5).

Continuity equation

$$\frac{\partial \rho}{\partial t} + \nabla \cdot (\rho \mathbf{v}) = 0 \quad (1)$$

Momentum equation

$$\frac{\partial \rho \mathbf{v}}{\partial t} + \nabla \cdot (\rho \mathbf{v} \times \mathbf{v}) - \nabla \cdot (\mu_{\text{eff}} \nabla \mathbf{v}) = -\nabla p + \nabla \cdot (\mu_{\text{eff}} \nabla \mathbf{v}) + S \quad (2)$$

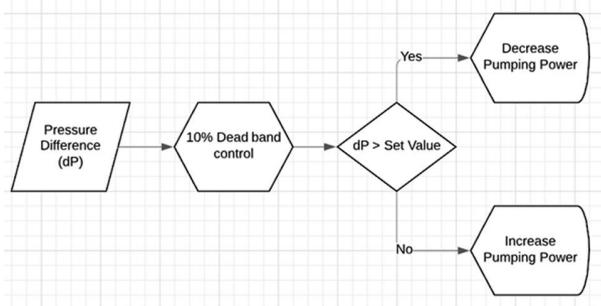


Fig. 3 Control system flowchart

Energy equation

$$\frac{\partial(\rho h)}{\partial t} - \frac{\partial(p)}{\partial t} + \nabla \cdot (\rho v h) = \nabla \cdot \left[\left(\mu + \frac{\mu_t}{\sigma_k} \right) \nabla h \right] - S_h \quad (3)$$

Turbulence equations

Turbulent energy equation

$$\frac{\partial(\rho k)}{\partial t} + \nabla \cdot (\rho v k) = \nabla \cdot \left[\left(\mu + \frac{\mu_t}{\sigma_k} \right) \nabla k \right] + G_k + G_b - \rho \varepsilon \quad (4)$$

Turbulence dissipation rate equation

$$\frac{\partial(\rho \varepsilon)}{\partial t} + \nabla \cdot (\rho v \varepsilon) = \nabla \cdot \left[\left(\mu + \frac{\mu_t}{\sigma_\varepsilon} \right) \nabla \varepsilon \right] + \frac{\varepsilon}{\lambda} (c_{\varepsilon 1} G_k - c_{\varepsilon 2} \rho \varepsilon) \quad (5)$$

2.5 Mesh sensitivity Analysis. A Mesh sensitivity analysis is done to determine the right grid for the analysis to have a good accuracy for the solution. 6SigmaET has the capability of adapting the grid based on the model [19]. A local gridding feature in the software is used to create enough grid to capture the heat transport. Based on Fig. 4, model uses around 2 million grid for all the simulations.

3 Flow Control Device Functionality

A MATLAB code was developed to mimic the functionality of FCD using the experimental data [20]. This functionality will be used in controlling the coolant flow rate in 6 Sigma based on the readings provided by the temperature sensor. Figure 5 shows FCD hysteresis curve that is plotted from MATLAB code. The hysteresis

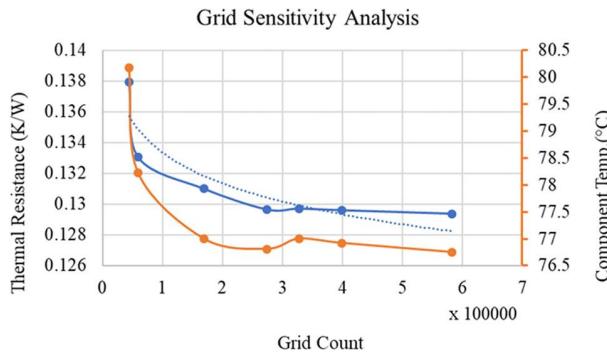


Fig. 4 Mesh sensitivity analysis

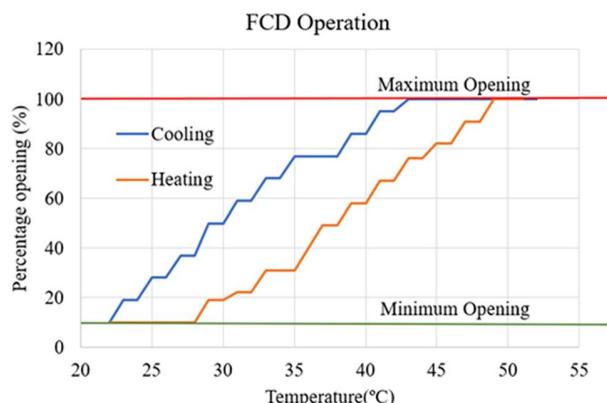


Fig. 5 FCD functionality

Table 1 Percentage of damper openings

| Pressure (Pa) | D1 | D2 | D3 | D4 |
|---------------|-------|-------|-------|-------|
| 300 | 28.31 | 40.12 | 69.98 | 64.86 |
| 400 | 18.02 | 20.25 | 24.3 | 24.08 |
| 500 | 13.42 | 14.64 | 17.69 | 17.63 |
| 600 | 10.84 | 11.33 | 13.96 | 13.97 |

Table 2 Temperature of the coolant at outlet of cold plate

| Pressure (Pa) | T1 (°C) | T2 (°C) | T3 (°C) | T4 (°C) |
|---------------|---------|---------|---------|---------|
| 300 | 37.11 | 37.12 | 37.38 | 37.28 |
| 400 | 36.92 | 37.02 | 37.11 | 37.12 |
| 500 | 36.99 | 36.93 | 36.94 | 36.95 |
| 600 | 36.95 | 36.97 | 37 | 37.01 |

between cooling and heating cycle of the fluid is observed as 4–6 °C. A minimum opening of 10% is by design to monitor the temperature changes in the fluid and cool the minimum utilization of the component. Numerous simulations are carried out to bring the harmony to the multicontrol integration.

4 Results and Discussion

4.1 System Pressure Drop Analysis. System pressure drop is calculated to provide the set point values for the control strategy. Table 1 shows the results for various pressure drops across the system and the damper response with the fixed flow rate and having the FCD maintaining the outlet temperatures at 37 °C. Table 1 shows some different damper opening values with same power. Four different values of pressure are tested to find out the pressure set point. The values D1, D2, D3, D4 indicate respective dampers for the cold plates 1, 2, 3, 4.

The values T1, T2, T3, T4 in Table 2 indicate the outlet temperatures of coolant at the respective cold plates 1,2,3,4. Table 1 shows that at 300 Pa the dampers are at different percentage of opening. This is not supposed to happen because the power dissipated by all the component is the same. Once the pressure is more than 400 Pa, the damper openings are relatively close to each other with a maximum difference of 6%. The distance of cold plate from the pump will also be affecting the pressure of the system and flow across each cold plate. The 300 Pa pressure drop has elevated outlet temperatures which are more than 37 °C, but the pressures more than 400 Pa have almost constant temperature outlet which is 37 °C. With 300 Pa the temperature rise is slightly higher than the set point value also the damper openings are very large that this will create imbalance when the powers are varying. Hence, 400 Pa is determined to be the required pressure for the system. The temperature values also agree with the damper openings. Based on these findings 400 Pa will be used as the pressure set point to control the pump.

4.2 Controls testing. The set point of pressure (400 Pa) value is used in the controls and is tested for different powers. Table 3 shows the iterations with different sets of power. U1, U2, U3 and U4 represent the power of the components with respective to the cold plates 1, 2, 3, 4. The power is varied from 100 to 400 W and the control strategy was applied to vary the pump flow rate based on the system pressure maintaining a constant pressure for the overall system. Flow rate at each cold plate is controlled by the FCD opening based on temperature outlet from the cold plate. Control strategy was tested using the sample set provided in Table 3, which covered all the possible power combinations required in the taken scenario. There might be 256 number of possible combinations and arrangements with duplicates but, all of them will have a similar total power with the selected sample set.

Table 3 Power variation in the test cases

| Test case no. | Component U1 | Component U2 | Component U3 | Component U4 | Total power |
|---------------|--------------|--------------|--------------|--------------|-------------|
| 1 | 100 | 100 | 100 | 100 | 400 |
| 2 | 100 | 100 | 100 | 200 | 500 |
| 3 | 100 | 100 | 100 | 300 | 600 |
| 4 | 100 | 100 | 100 | 400 | 700 |
| 5 | 100 | 100 | 300 | 300 | 800 |
| 6 | 100 | 100 | 300 | 400 | 900 |
| 7 | 100 | 200 | 300 | 400 | 1000 |
| 8 | 200 | 200 | 300 | 400 | 1100 |
| 9 | 200 | 300 | 300 | 400 | 1200 |
| 10 | 200 | 300 | 400 | 400 | 1300 |
| 11 | 200 | 400 | 400 | 400 | 1400 |
| 12 | 300 | 400 | 400 | 400 | 1500 |
| 13 | 400 | 400 | 400 | 400 | 1600 |

These samples are simulated and the data on flow rate, temperature, damper openings, and pressure drops are collected for processing.

4.3 Pumping Power. Pumping power is equal to the product of flow rate and pressure drop of the system [16]. In this study, pumping power for all the scenarios is calculated based on their respective flow rates with the applied control strategy. As shown in Fig. 6, the pumping power changes based on the system power as FCDs are installed. Pump flow rate will be changed according to the overall system requirements whereas the FCDs will control the individual flow rate at the cold plate level. In a none FCD scenario, the pumping power will be constant and is directly proportional to the maximum junction temperature of the highest-powered component in the overall system. The green line on top of the chart in Fig. 6 represents the fixed pumping power line. In the application of this solution a centrifugal pump with a VFD should be able to maintain the pressure and provide the required flow rate. The PWM-type VFD normally uses a constant voltage which is pulsed with integrated bi-polar power transistors (IGBT). The sine wave is generated by varying the width of the pulses. The frequency with which the transistors are turned on and off is called switching frequency. The higher the switching frequency, the better the reproduction of the ideal sine wave [21]. Using this PWM signal, we can maintain the required flow rate at all times as well as reduce the pumping power based on the demand for cooling.

4.4 Pumping Power Savings. Figure 7 shows that there is potential for saving the pumping power up to 64%, when compared to fixed pumping power. The comparison of liters per minute/kW between the two cases with and without FCD suggests

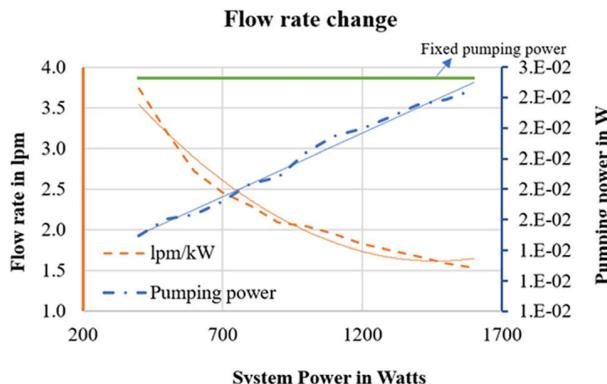


Fig. 6 Pressure versus outlet temperatures for different components

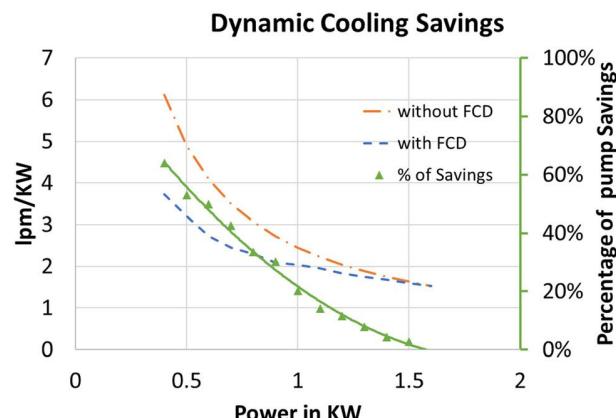


Fig. 7 Pumping power savings

that having an FCD will reduce the flow rate requirements. This reduces the pumping power with the help of a VFD controlled pump.

4.5 Partial Power Usage Effectiveness. Power usage effectiveness has been widely adapted and used throughout as a standard efficiency metric for data centers. PUE is determined as the total power consumed by the data center divided by the power consumed by the IT load (useful work of the data center). Partial PUE (pPUE) metrics can be developed to understand the efficiency of specific subsystems and subsets of the data center. pPUE of cooling systems can be expressed as shown in Eq. (6). Based on the power consumption of the pump, the PUE will be varying. With the test scenarios shown in the results we are able to observe the PUE varying between 1.007 and 1.01. This is only due to pumping power change.

$$p\text{PUE}_{\text{cooling}} = \frac{(\text{Cooling Power} + \text{Server Load})}{(\text{Server Power})} \quad (6)$$

5 Conclusion

Implementation of a DCP is effective with a good control strategy. In this study, a novel control strategy was developed and tested to save overall pumping power at a rack and data center level. The control strategy developed is tested using simulations in 6SigmaET. Pressures are calculated for individual components at 100% possible flow rate, and then cumulative pressure is given as a pressure boundary condition to the system for the methodology adopted. The controls are optimized to have only single sensor input to control the VFD pump. Various possible powers are varied and tested to show how dynamic cooling and FCD help

save the pumping power. It is proven that the control strategy is fully functional with the test setup developed in 6SigmaET. It is shown that there is potential for saving the pumping power up to 64%, when compared to fixed pumping power. This helps us to conclude that dynamic cooling along with the control strategy is an efficient cooling solution for IT equipment cooling.

Acknowledgment

Immeasurable appreciation and deepest gratitude for the help and support are extended to everyone who have contributed in making this study possible. Deserving of special mention are Future Facilities 6SigmaET without whose resources this project would not be possible.

Funding Data

- NSF IUCRC (No. IIP-1738811; Funder ID: 10.13039/100000001).

Nomenclature

- p = pressure (Pa)
 v = velocity (m/s)
 $c\varepsilon_1 = 1.44$
 $c\varepsilon_2 = 1.92$
 ε = turbulent dissipation rate (m^2/s^2)
 G_b, G_k = turbulence kinetic energies (m^2/s^2)
 μ = viscosity ((Ns)/ m^2)
 h = enthalpy of the fluid (J)
 μ_{eff} = effective viscosity ((Ns)/ m^2)
 k = turbulence kinetic energy (m^2/s^2)
 μ_t = turbulence viscosity ((Ns)/ m^2)
 S = source term
 ρ = density (kg/m^3)
 Sh = volumetric heat source ($kJ/(m^3 s)$)
 $\sigma\varepsilon = 1.2$
 $\sigma k = 1$
 $\sigma t = \text{constant}$
 t = time (h)
 T = temperature ($^\circ C$)

References

- [1] Margaret Rouse, 2019, "What is a Data Center?," Data Center, Newton, MA, accessed Sept. 6, 2020, <https://searchdatacenter.techtarget.com/definition/data-center>
- [2] Shah, J. M., Eiland, R., Rajmane, P., Siddarth, A., Agonafer, D., and Mulay, V., 2019, "Reliability Considerations for Oil Immersion-Cooled Data Centers," *ASME J. Electron. Packag. Trans.*, **141**(2), p. 021007.
- [3] Ramdas, S., Rajmane, P., Chauhan, T., Misrak, A., and Agonafer, D., 2019, "Impact of Immersion Cooling on Thermo-Mechanical Properties of PCB's and Reliability of Electronic Packages," *ASME Paper No. IPACK2019-6568*.
- [4] Eiland, R., Fernandes, J., Vallejo, M., Agonafer, D., and Mulay, V., 2014, "Flow Rate and Inlet Temperature Considerations for Direct Immersion of a Single Server in Mineral Oil," Fourteenth Intersociety Conference on Thermal and Thermomechanical Phenomena in Electronic Systems (ITherm), Orlando, FL, May 27–30, pp. 706–714.
- [5] Almoli, A., Thompson, A., Kapur, N., Thompson, H., and Hannah, G., "Computational Fluid Dynamic Investigation of Liquid Rack Cooling in Data Centres," *Appl. Energy*, **89**(1), pp. 150–155.
- [6] Ellsworth, Jr., M. J., and Iyengar, M. K., 2009, "Energy Efficiency Analyses and Comparison of Air and Water Cooled High Performance Servers," *ASME Paper No. InterPACK2009-89248*.
- [7] Fernandes, J., Ghalmamor, S., Agonafer, D., Kamath, V., and Schmidt, R., 2012, "Multi-Design Variable Optimization for a Fixed Pumping Power of a Water-Cooled Cold Plate for High Power Electronics Applications," *13th InterSociety Conference on Thermal and Thermomechanical Phenomena in Electronic Systems, ITherm*, San Diego, CA, May 30–June 1, pp. 684–692.
- [8] Zimmermann, S., Meijer, I., Tiwari, M. K., Paredes, S., Michel, B., and Poulikakos, D., 2012, "Aqasar: A Hot Water Cooled Data Center With Direct Energy Reuse," *Energy*, **43**(1), pp. 237–245.
- [9] Chu, R. C., Hwang, U. P., and Simons, R. E., 1982, "Conduction Cooling for an LSI Package: A One-Dimensional Approach," *IBM J. Res. Dev.*, **26**(1), pp. 45–54.
- [10] American Society of Heating, Refrigerating and Air-Conditioning Engineers (ASHRAE), 2009, "Best Practices for Datacom Facility Energy Efficiency," ASHRAE, Atlanta, GA.
- [11] Fernandes, J. E., 2015, "Minimizing Power Consumption at Module, Server and Rack-Levels Within a Data Center," *Ph.D. thesis*, The University of Texas at Arlington, Arlington, TX.
- [12] Kasukurthy, R., Challa, P. S., Palanikumar, R. R., Manimaran, B. R., and Agonafer, D., 2018, "Flow Analysis and Linearization of Rectangular Butterfly Valve Flow Control Device for Liquid Cooling," *Proceedings of the 17th InterSociety Conference on Thermal and Thermomechanical Phenomena in Electronic Systems, ITherm 2018*, San Diego, CA, May 29–June 1, pp. 683–687.
- [13] Kasukurthy, R., 2019, "Design and Optimization of Thermal Management Approaches in Data Center Application," *Ph.D. thesis*, The University of Texas at Arlington, Arlington, TX.
- [14] Chowdhury, U., Sahini, M., Siddarth, A., Agonafer, D., and Branton, S., 2017, "Characterization of an Isolated Hybrid Cooled Server With Failure Scenarios Using Warm Water Cooling," *ASME Paper No. IPACK2017-74028*.
- [15] Sahini, M., Kshirsagar, C., Kumar, M., Agonafer, D., Fernandes, J., Na, J., Mulay, V., McGinn, P., and Soares, M., 2017, "Rack-Level Study of Hybrid Cooled Servers Using Warm Water Cooling for Distributed vs. centralized Pumping Systems," *2017 33rd Thermal Measurement, Modeling & Management Symposium (SEMI-THERM)*, San Jose, CA, Mar. 13–17, pp. 155–162.
- [16] Currie, I. G., 2016, *Fundamental Mechanics of Fluids*, CRC Press, Boca Raton, FL.
- [17] Versteeg, H. K., and Malalasekera, W., 1995, *An Introduction to Parallel Computational Fluid Dynamics: The Finite Volume Method*, Pearson, London, UK.
- [18] Kim, D., and Oh, S., 2018, "Optimizing the Design of a Vertical Ground Heat Exchanger: Measurement of the Thermal Properties of Bentonite-Based Grout and Numerical Analysis," *Sustainability*, **10**(8), pp. 1–17.
- [19] Future Facilities 6Sigma, 2019, "User Guide, Future Facilities 6Sigma Version 13.0," Future Facilities 6Sigma, San Jose, CA, accessed Sept. 6, 2019, <https://user.login.futurefacilities.com/index.php?sid=5b7089657c16af4a77848e9a49ff0c041>
- [20] Palanikumar, R. R., 2018, "Experimental and Analytical Study of a Self-Regulated Flow Control Device Developed for Dynamic Cold-Plates to Cool High-Power Density Multi-Chip Modules," *MS thesis*, The University of Texas at Arlington, Arlington, TX.
- [21] ITT Industries, 2019, "Variable Frequency Drive Recommendations," ITT Industries, New York, accessed Dec. 21, 2019, https://www.gsengr.com/uploaded_files/Variable_Frequency_Drive_Recommendations_For_Centrifugal_Pumps.pdf